Excitons in semiconductor quantum discs

2001 J. Phys.: Condens. Matter 13 1485

(http://iopscience.iop.org/0953-8984/13/7/311)

INSTITUTE OF PHYSICS PUBLISHING JOURNAL OF PHYSICS: CONDENSED MATTER

J. Phys.: Condens. Matter **13** (2001) 1485–1498 www.iop.org/Journals/cm PII: S0953-8984(01)15571-2

Excitons in semiconductor quantum discs

Tong San Koh[1], Yuan Ping Feng[2], Xin Xu[2] and Harold N Spector[3]

[1] Centre for Advanced Numerical Engineering Simulation, Nanyang Technological University, 639798 Singapore
[2] Department of Physics, National University of Singapore, 119260 Singapore
[3] Department of Physics, Illinois Institute of Technology, Chicago, IL 60616, USA

Received 13 July 2000, in final form 4 January 2001

Abstract

The ground-state binding energy of the exciton in a finite-potential quantum disc setting is calculated variationally to study the change in dimensionality of the exciton within the limiting cases of the quantum well, wire, and dot, as well as the intermediate regime between these limiting geometries. Quantitative comparisons have been made with previous calculations using different trial wavefunctions to show the superiority of the present trial wavefunction in the quantum disc setting and to further illustrate the behaviour of the exciton in the quantum dot limit. Using the binding energy obtained from the present calculations, we further calculated the virial theorem number for the exciton in various confinement geometries, to disprove the recent claim of the existence of universal-constant virial theorem numbers for the quantum wells and wires. Also, the dimensionality parameter of the fractional-dimensionality model for confined excitons in the various confinement geometries has been calculated to facilitate discussion of its applicability to these structures, including the quantum dot limit.

1. Introduction

It is well established that the confinement of excitons in quantum wells yields enhanced excitonic effects (such as the binding energy and oscillator strength) which can be exploited in the design of novel optoelectronic devices. Advances in nanoscale fabrication techniques have further brought about the reduction of the effective dimension of excitonic states—from quasi-two-dimensional (2D) down to the quasi-one-dimensional (1D) and 'zero'-dimensional (0D) states. The question of whether excitonic states are even more enhanced and the extent of the enhancement in these reduced-dimensional ($<$2D) structures has thus been a topic of much interest in the past few years [1–15]. In view of the rapid development in crystal growth and fabrication techniques, as we progress from microtechnologies to nanotechnologies whereby devices are designed in the nanometre range, it becomes increasingly necessary to address the concern of the exciton losing its enhanced effects in the ultrasmall quantum structures, due to the increased penetration of the exciton wavefunction into the barrier regions in the direction of diminishing spatial confinement. The exciton binding energy typically increases

with the initial decrease in spatial confinement to reach a peak at some critical confinement width (which is dependent on the height of the potential barrier), then decreases with further decrease in confinement width when the exciton wavefunction extends substantially into the barrier regions and recovers a higher dimensionality. This implies that there exists certain critical confinement limit where the quantum confinement effect is a maximum, beyond which the bulk effect sets in again. Hence, the concern in the near future will be to determine not only the length scale on which the quantum confinement effects would become appreciable with the decrease in spatial confinement, but also when these enhanced effects would be lost. The estimation and understanding of this critical confinement limit in quantum 2D, 1D, and 0D structures is hence of relevance.

Recently, there has also been growing interest in two topics regarding the confined excitonic states. The first is the fractional-dimensional model of the confined exciton [16–21], and the second is the possible existence of universal virial theorem numbers [22–24] of confined excitons in the various quantum structures. A common reason for the interest in these two topics is the possible simplification of the intensive computation involved in obtaining exciton binding energies in the quantum structures, especially in the wire and dot. In the model of fractional-dimensional space, He [16–18] proposed that the Wannier–Mott excitons in an anisotropic solid can be treated as ones in an isotropic fractional-dimensional space, where the dimension is deformed by the degree of anisotropy. The anisotropic interaction in 3D space then becomes isotropic in a lower-fractional-dimensional space. In this space, the confined exciton problem returns to one of a fractional-dimensional hydrogenic Schrödinger equation with discrete exciton bound-state energies (E_n) given by

$$E_n = E_g - \frac{\text{Ryd}}{\left[n + (\alpha_f - 3)/2\right]^2} \tag{1}$$

where E_g is the band-gap energy, $n = 1, 2, \ldots$ is the principal quantum number, and Ryd is the 3D exciton Rydberg energy. Here, only a single parameter, α_f (known as the degree of dimensionality), is needed to incorporate the effect of change in the confinement geometry on the strength of the interaction; and setting $\alpha_f = 3$, 2, and 1 leads to the well-known integer-dimensional results. Using equation (1) the estimation of the exciton energy boils down to the approximation of α_f. This approach has been adopted by Christol *et al* [19, 20] in their calculations of the exciton binding energies in quantum well and wires, which yield reasonable results as compared with the more computationally intensive methods. Also, α_f has been employed to estimate the Stark shift in exciton complexes in quantum wells [21]. According to the fractional-dimensional model, other quantities, such as the exciton effective radius and oscillator strength in the various quantum structures, can also be calculated from simple equations involving α_f [16–20].

As for the virial theorem for confined excitons, recently Rossi *et al* [22] found that in the strong-confinement limit, the same potential-to-kinetic-energy ratio holds for quite different wire cross-sections and compositions. This ratio (=4) is found to be twice the value imposed by the conventional virial theorem for 3D and 2D systems. If such a scaling rule does exist for excitons in these quantum structures, it can be exploited in simplifying the calculations of the confined excitonic states, as in the calculations of Thilagam [23]. The virial theorem states that for an interaction potential of the form

$$V(r_{ij}) = \sum_{ij} a_{ij} r_{ij}^{v}$$

between two charges i and j (where $r = |\vec{r}_i - \vec{r}_j|$ and the as are constants), the relation between

the kinetic (T), potential (V), and binding (E_b) energies is given by

$$T = \frac{v}{2+v}E_b = \frac{v}{2}V.$$

If the virial theorem number, v, is known to be some fixed universal value, then the effective potential describing the interaction between the electron and hole in an electron–hole pair can be approximated in the form $V_{eff} \sim -r^v$ which may differ from the usual Coulombic form for 3D and 2D systems. A simplified exciton model whereby the exciton is solely governed by this effective potential can then be used for strongly confined systems.

In the present work, we study the exciton in a quantum disc in regard to the above concerns and subjects, using a variational approach and the effective-mass approximation with a finite-confinement-potential model. As proposed by Kayanuma [3], by varying the radius (R) and width/height (L) of the quantum disc/cylinder, the quantum disc arrangement allows one to systematically explore the various limiting situations of the bulk (for R and $L \gg a_B$, where a_B is the 3D exciton Bohr radius), the quantum well (for $R \gg a_B$ and $L < a_B$), the quantum wire (for $R < a_B$ and $L \gg a_B$), and the quantum dot (for $R < a_B$ and $L < a_B$), as well as the transition in the intermediate regime of these limits in a continuous, 'unified' manner. Here, we are also interested in the dimensionality crossover in the critical confinement limit where quantum confinement effects are rapidly overwhelmed by the bulk effect. Although previous work [5–7] has been done on the variational calculation of the exciton in the quantum disc, the authors have used different trial wavefunctions which have their individual limitations for certain geometries of the disc. Also there seems to be a lack as regards comparison and justification of these wavefunctions employed in quantum disc calculations, as the success and accuracy of results based on variational methods often depend on the parameters chosen and the functional form of the trial wavefunction used. Here we use a superior trial wavefunction which can account for the correct behaviour of the exciton in the limiting geometries where the previous trial wavefunctions fail, to quantitatively study and compare them. There have been concerns as to whether the effective-mass approximation could still be valid in the quantum dot limit when the size of the exciton could be of the order of the average lattice constants of the bulk semiconductor. Recently, Marin *et al* [25] performed variational calculations of the exciton energies for spherical dots of radius in the range of 5–40 Å to compare with both experimental and other theoretical data for CdS, CdSe, PbS, and CdTe crystallites; and they found that the effective-mass approximation is still appropriate for those geometries. Moreover, in the limit of very small spatial confinement where the exciton extends substantially into the barrier material, the effective-mass approximation could again be an appropriate approximation with the exciton described by the effective mass of the embedding barrier material. Using the exciton binding energy and wavefunction obtained variationally, we further proceed to calculate the virial theorem number and the fractional-dimensional parameter for a wide range of quantum discs and cylinders which are representative of the various limiting confinement situations. The validity of the virial theorem conjecture of Rossi *et al* [22] and the applicability of the fractional-dimensional parameter for these quantum structures are then systematically studied and discussed.

2. Model calculation

Here, we adopt a coordinate system similar to those used in previous works [5–7]. For completeness, we show the coordinate arrangement and orientation in figure 1. The in-plane coordinates on the circular cross-section of the disc/cylinder are denoted by r_c where $c = e, h$ for the electron and hole respectively; and the cylinder axis is taken as the z-axis.

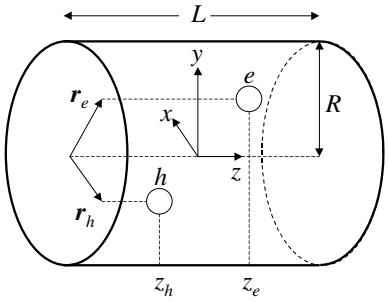

Figure 1. The various coordinates in the quantum disc arrangement. The r_cs denote the in-plane coordinates and the z_cs denote the positions along the disc/cylinder axis.

2.1. Single-particle ground state

We first consider the ground state of a single particle in the quantum disc within the framework of the effective-mass and envelope function approximations. For compactness, we use the following notation for the mass of the particle:

$$m_c^{\parallel}(r_c) = m_c\theta(R - r_c) + m_c'\theta(r_c - R) \tag{2a}$$

$$m_c^{\perp}(z_c) = m_c\theta\left(\frac{L}{2} - |z_c|\right) + m_c'\theta\left(|z_c| - \frac{L}{2}\right). \tag{2b}$$

Here, m_c and m_c' refer to the particle's effective masses in the disc and barrier materials, respectively; and θ is the Heaviside step function.

If we consider separately the in-plane and z-axis motions of the particle confined by the potentials

$$V_c^{\parallel}(r_c) = \begin{cases} 0 & \text{if } r_c < R \\ V_c & \text{otherwise} \end{cases} \tag{3a}$$

and

$$V_c^{\perp}(z_c) = \begin{cases} 0 & \text{if } |z_c| < L/2 \\ V_c & \text{otherwise} \end{cases} \tag{3b}$$

respectively, the corresponding 2D and 1D effective-mass Schrödinger equations are

$$\left\{-\frac{\hbar^2}{2m_c^{\parallel}}\nabla_c^2 + V_c^{\parallel}(r_c)\right\} f_c(r_c) = E_c^{\parallel} f_c(r_c) \tag{4a}$$

$$\left\{-\frac{\hbar^2}{2m_c^{\perp}}\nabla_c^2 + V_c^{\perp}(z_c)\right\} g_c(z_c) = E_c^{\perp} g_c(z_c) \tag{4b}$$

with ground-state solutions of the form

$$f_c(r_c) = \begin{cases} J_0(\theta_c r_c) & r_c \leqslant R \\ B_c K_0(\beta_c r_c) & r_c > R \end{cases} \tag{5a}$$

$$g_c(z_c) = \begin{cases} \cos(k_c z_c) & |z_c| \leqslant L/2 \\ A_c \exp(-q_c|z_c|) & |z_c| > L/2. \end{cases} \tag{5b}$$

Here, in view of the mass mismatch, θ_c, β_c, k_c, and q_c are determined from the following boundary conditions

$$\frac{1}{m_c}\frac{1}{f_c(r_c<R)}\frac{\partial f_c(r_c<R)}{\partial r_c}\bigg|_{r_c=R} = \frac{1}{m_c'}\frac{1}{f_c(r_c>R)}\frac{\partial f_c(r_c>R)}{\partial r_c}\bigg|_{r_c=R} \tag{6a}$$

$$\frac{1}{m_c}\frac{1}{g_c(|z_c|<L/2)}\frac{\partial g_c(|z_c|<L/2)}{\partial z_c}\bigg|_{z_c=L/2} = \frac{1}{m_c'}\frac{1}{g_c(|z_c|>L/2)}\frac{\partial g_c(|z_c|>L/2)}{\partial z_c}\bigg|_{z_c=L/2}. \tag{6b}$$

Equations (6*a*) and (6*b*) are obtained by requiring the respective wavefunctions and their flux densities to be continuous at the interfaces with the barrier material. The Ben Daniel–Duke model [26] is used because of its simplicity. For the full 3D motion, the product $f_c(r_c)g_c(z_c)$ is no longer a solution of the 3D effective-mass Schrödinger equation since the actual 3D finite confinement potential is not straightforwardly the sum of the finite confinements $V_c^{\parallel} + V_c^{\perp}$. Using the perturbational approach suggested by the Le Goff and Stebe [5,6], we write the 3D finite confinement potential as

$$V_c(\vec{r}_c) = V_c^{\parallel}(r_c) + V_c^{\perp}(z_c) + \delta V_c(r_c, z_c) \tag{7}$$

where

$$\delta V_c = \begin{cases} 0 & \text{if } r_c < R \text{ and } |z_c| < L/2 \\ -V_c & \text{otherwise} \end{cases} \tag{8}$$

is treated as a perturbation potential. The ground-state energy of a particle in the quantum disc with finite confinement can then be approximated by

$$E_c = E_c^{\parallel} + E_c^{\perp} - \frac{\langle f_c g_c|\delta V_c|f_c g_c\rangle}{\langle f_c g_c|f_c g_c\rangle}. \tag{9}$$

2.2. Exciton ground state

Using the relative coordinate $r = |\vec{r}_e - \vec{r}_h| = (r_e^2 + r_h^2 - 2r_e r_h\cos\theta)^{1/2}$, the model Hamiltonian of the exciton can be written as

$$\begin{aligned} H = &-\frac{\hbar^2}{2m_e^{\parallel}}\left\{\frac{\partial^2}{\partial r_e^2} + \frac{1}{r_e}\frac{\partial}{\partial r_e} + \frac{r_e^2 - r_h^2 + r^2}{r_e r}\frac{\partial^2}{\partial r_e\,\partial r}\right\} \\ &- \frac{\hbar^2}{2m_h^{\parallel}}\left\{\frac{\partial^2}{\partial r_h^2} + \frac{1}{r_h}\frac{\partial}{\partial r_h} + \frac{r_h^2 - r_e^2 + r^2}{r_h r}\frac{\partial^2}{\partial r_h\,\partial r}\right\} - \frac{\hbar^2}{2\mu}\left\{\frac{\partial^2}{\partial r^2} + \frac{1}{r}\frac{\partial}{\partial r}\right\} \\ &- \frac{\hbar^2}{2m_e^{\perp}}\frac{\partial^2}{\partial z_e^2} - \frac{\hbar^2}{2m_h^{\perp}}\frac{\partial^2}{\partial z_h^2} + V_e(r_e, z_e) + V_h(r_h, z_h) - \frac{e^2}{\epsilon\sqrt{r^2 + (z_e - z_h)^2}} \end{aligned} \tag{10}$$

where $\mu(r_e, r_h)^{-1} = m_e^{\parallel}(r_e)^{-1} + m_h^{\parallel}(r_h)^{-1}$ is the in-plane reduced mass of the exciton and ϵ is the dielectric constant. We have assumed that the wavefunction is independent of θ in deriving equation (10). Polarization and image charge effects due to dielectric mismatch can be significant when there is a large dielectric discontinuity between the quantum structure and the surrounding medium, as in the case of 'free-standing' vacuum/GaAs/vacuum quantum structures [15]. Although the image charge effects has been found to enhance the binding energy of excitons in the $Ga_{1-x}Al_xAs$ quantum wells (by not more than 1 meV) [10], Banyai *et al* [2] have shown that this polarization effect could be reduced in the quantum wire as compared with the quantum well. They performed their calculations using a wire-to-barrier dielectric constant ratio of 1.3 for $Ga_{1-x}Al_xAs$, and since the materials commonly used for the

manufacture of $Ga_{1-x}Al_xAs$ quantum wires have a dielectric constant ratio less than 1.3, they have neglected such effects in their subsequent calculations [2]. Hence, we believe that the present simplified model could still give a reasonable approximation of the exciton behaviour in the $Ga_{1-x}Al_xAs$ quantum cylinder.

Here, we adopt the variational approach to estimate the ground-state exciton binding energy and wavefunction. As in the previous works, we may choose a trial wavefunction of the following form:

$$\psi_{ex} = F_e(r_e, z_e)F_h(r_h, z_h)\phi(r, z_e, z_h) = f_e(r_e)g_e(z_e)f_h(r_h)g_h(z_h)\phi(r, z_e, z_h) \tag{11}$$

where $\phi(r, z_e, z_h)$ is the relative wavefunction describing the internal motion of the electron–hole pair. Previously, two different relative wavefunctions have been used in the variational calculation for the ground-state exciton in the quantum disc. Kayanuma [3] employed the isotropic hydrogenic wavefunction *ansatz*

$$\phi_1(r, z_e, z_h) = \exp\left[-\alpha\sqrt{r^2 + (z_e - z_h)^2}\right] \tag{12}$$

with a single variational parameter, α. Although this wavefunction should be good in the limit of large R and L or when an isotropic behaviour is expected, it may not be adequate in situations when the exciton is highly anisotropic, such as in a narrow quantum well or thin quantum wire. It should be noted that even with this simplified wavefunction, the variational treatment required numerical evaluation of fourfold integrals before the single-parameter energy minimization (with respect to α), which hence imposes a heavy computational burden. Later, Le Goff and Stebe [5, 6] introduced a two-parameter relative variational wavefunction:

$$\phi_2(r, z_e, z_h) = \exp[-\alpha r]\exp[-\gamma(z_e - z_h)^2] \tag{13}$$

in an attempt to avoid the occurrence of the fourfold integrals, and to account for possible anisotropy; and Susa [7] adopted the same wavefunction and included the effective-mass mismatch which was ignored in [5, 6]. However, we note that this wavefunction is separable in the in-plane and z-coordinates and cannot reproduce the proper 3D hydrogenic wavefunction in the bulk limit where the exciton is isotropic. Hence the above two trial wavefunctions have their individual limitations, in the sense that they may only be good for certain ranges of R and L. Also, to the best of our knowledge, no quantitative comparisons have been made between the results given by these two trial wavefunctions for the quantum disc.

In the present calculation, we use the following anisotropic two-parameter relative wavefunction which has proved to be superior for quantum well structures:

$$\phi_3(r) = \exp\left[-\alpha\sqrt{r^2 + \gamma(z_e - z_h)^2}\right]. \tag{14}$$

The form of this *ansatz* not only satisfies the anisotropy requirements, but also yields the correct hydrogenic form in the bulk limit. We also note that ϕ_1 is a special case of the more general ϕ_3, and that the fourfold numerical integrations will still have to be performed, together with a two-parameter minimization, which hence leads to a much heavier computational burden.

The ground-state energy and wavefunction can be determined by minimizing the exciton energy functional

$$\langle E_{ex}(\alpha, \gamma)\rangle = \frac{\langle\psi_{ex}|H|\psi_{ex}\rangle}{\langle\psi_{ex}|\psi_{ex}\rangle} \tag{15}$$

with respect to both α and γ. The binding energy is defined by

$$E_b = E_e + E_h - E_{ex}. \tag{16}$$

Once the binding energy is obtained, we may proceed to calculate the virial theorem number

$$v = -\frac{E_C}{E_K} \tag{17}$$

where $E_C = \langle -e^2/\epsilon\sqrt{r^2 + (z_e - z_h)^2}\rangle$ is the Coulombic energy term evaluated using the optimized parameters α and γ; and E_K is the kinetic energy term.

The binding energy in the fractional-dimensional model is given by the second term on the right-hand side of equation (1). For the ground-state exciton, $n = 1$, and α_f can be calculated from

$$\alpha_f = 1 + 2\left(\frac{\text{Ryd}}{E_b}\right)^{1/2} \tag{18}$$

after some rearrangement.

3. Results and discussion

In order to make quantitative comparisons of the binding energies obtained using different trial wavefunctions, we have performed variational calculations using the isotropic wavefunction ϕ_1 in equation (12) and the two-parameter anisotropic wavefunction ϕ_3 (equation (14)) to allow comparison with the results previously obtained by Susa [7] using the two-parameter separable wavefunction, ϕ_2 (equation (13)). We have hence adopted the same $Ga_{0.7}Al_{0.3}As$ material parameters as Susa [7]. The effective masses for the electron and heavy hole for $Ga_{1-x}Al_xAs$ are respectively $m_e = 0.0665 + 0.0835x$ and $m_h = 0.34 + 0.42x$ in units of the free-electron mass, with the dielectric constant $\epsilon = 13.18 - 3.12x$. The band-gap energy is

$$E_g = \begin{cases} 1.424 + 1.247x & 0 < x < 0.45 \\ 1.424 + 1.247x + 1.147(x - 0.45)^2 & 0.45 < x < 1.0 \end{cases} \tag{19}$$

and a 65–35 ratio is assumed between the conduction band and valence band offsets. Using these material parameters, the 3D Rydberg is Ryd = 5.048 meV and the 3D Bohr radius is given by $a_B = 116.50$ Å for the heavy-hole exciton.

3.1. Exciton binding energy

Figure 2 shows the calculated exciton binding energy as a function of the radius of the quantum disc R for widths L of 70 Å and 100 Å. We choose to compare these two values of L with the results of Susa [7], as it was explained by Le Goff and Stebe [5, 6] that the separable wavefunction, ϕ_2, is expected to be a good approximation in the limit of strong quantum confinement and when $L/R < 1$. From figure 2, we see that both ϕ_1 and ϕ_3 yield consistently higher binding energies than ϕ_2. This means that both ϕ_1 and ϕ_3 give lower exciton energies (E_{ex}) than ϕ_2, and in a variational sense, implying that they are better trial wavefunctions. We also note that for smaller R-values, the difference between the binding energies given by ϕ_2 and ϕ_3 becomes larger, while the binding energies given by ϕ_1 converge towards those of ϕ_3. It is interesting to note that even though ϕ_2 has two variational parameters, it could not perform better than ϕ_1 variationally. We believe that one possible reason is its separable form. As a result of the separable *ansatz*, using ϕ_2, integrations over certain coordinates can be analytically performed independently of the others, thus reducing the numerical cost of computations. The exciton energy functional can then be written as the sum of terms which are also separable functions of the in-plane coordinates (with α) and z-coordinates (with γ), except for the Coulombic term, which is treated by an asymptotic approximation approach

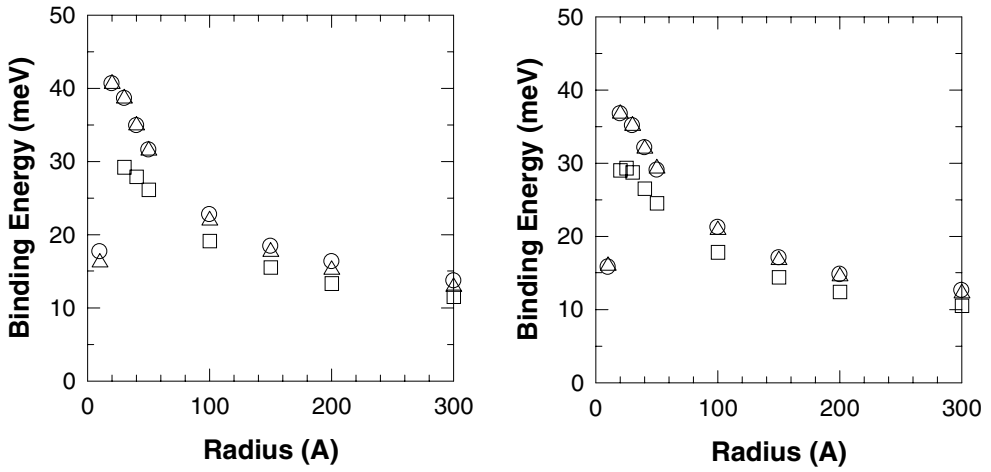

Figure 2. The exciton binding energy in the quantum disc is shown as a function of the disc radius R, for disc widths of (a) $L = 70$ Å and (b) $L = 100$ Å. The circles represent the current results obtained using ϕ_3, the triangles represent the results obtained using ϕ_1, and the squares represent the results obtained using ϕ_2 from reference [7].

(see equation (44) in reference [5]). Physically, such an energy expression seems to imply a largely 'separable behaviour' of the exciton. However, the success of the variational method depends on choosing a trial function which incorporates the correct qualitative features of the state. This probably also explains the larger deviation of the binding energies obtained for smaller R-values (with the diameters of the discs comparable to the widths), where the separable wavefunction and energy assumptions become less valid. On the other hand, ϕ_1 performs better in this range (i.e. yields results closer to ϕ_3), again indicating a rather isotropic behaviour of the exciton. Hence, considering that heavier computation is required for ϕ_3 than for ϕ_1, and the relatively small difference between the binding energies given by these two trial wavefunctions, we may say that ϕ_1 should still be a good trial wavefunction for the ground-state exciton in the quantum dot limit.

Figure 3 displays the transition of the exciton binding energies between quantum discs of various values of R and L, obtained using the present $Ga_{1-x}Al_xAs$ material parameters. We first compare the present results with the more familiar cases of the quantum well and wire. For the quantum discs with large values of R ($\sim$300 Å) which should approach the case of the quantum well, the binding energy as a function of L ranges from about 9.57 meV (1.89 Ryd) at $L = 300$ Å to a peak value of 15.12 meV (2.99 Ryd) at $L \simeq 30$ Å. These values are still slightly higher than those typical of quantum wells of the same L, indicating that the in-plane confinement still has an effect on the exciton. For the quantum cylinders of large L ($\sim$300 Å) and $R < 100$ Å which approach the situation of the quantum wire, the binding energy reaches a peak value of 26.28 meV (5.21 Ryd) at $R \simeq 20$ Å, which is again higher than previous $Ga_{1-x}Al_xAs$ quantum wire calculations [4, 20]. However, here we note that the binding energy decreases rather quickly with a further increase in L, and should approach a smaller value for a larger L closer to the quantum wire limit. For the smaller values of R and L ($\lesssim$100 Å), the binding energy increases sharply to reach a high value of 46.21 meV (9.15 Ryd) at $R \simeq 20$ Å and $L \simeq 30$ Å. This is the strong-confinement regime of the cylindrical quantum dot where the exciton is severely restricted in all spatial directions and quantum confinement

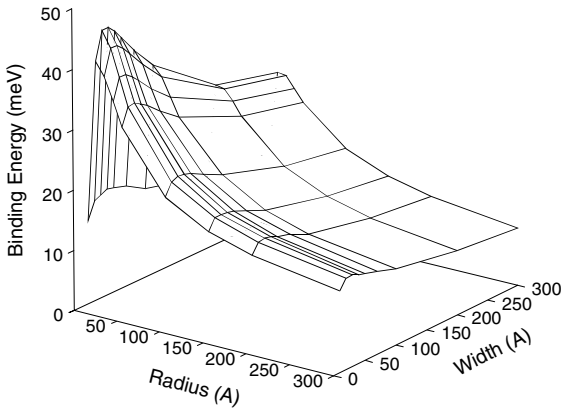

Figure 3. The exciton binding energy in the quantum disc is shown for various values of disc radius (R) and width (L) to illustrate the transition between the various confinement geometries representative of the quasi-3D, quasi-2D, quasi-1D, and quasi-0D cases.

effects are maximum. Due to the limitations of the previous separable trial wavefunction [5–7], such a high value of the exciton binding energy in the quantum disc has not been achieved variationally in the past using the finite-potential model. The present results again support the belief that the excitonic states should be enhanced and are more stable in a quantum dot than the wire and well.

It is worth noting that the binding energy approaches the bulk limit towards the four corners of the binding energy surface plot in figure 3, and except for that approaching large R and L (=300 Å), the corners are representative of the dimensionality crossovers where the bulk effect sets in. Also, for extremely small widths of $L \lesssim 30$ Å, and finite $R \sim a_B$, the quasi-1D situation is restored as the exciton is again becoming unconfined along the cylinder axis. Similarly, for the ultrasmall-R but finite-L limit ($R \lesssim 20$ Å and $L \sim a_B$), we again have a quasi-2D situation, as the exciton extends into the barrier regions along the in-plane directions and is confined only along the z-axis. We note that although the effective-mass boundary conditions in equation (6) allow the exciton to be described in terms of the different masses of the disc and barrier materials, such an exciton in the ultrasmall R but finite-L limit has two of its spatial dimensions largely described by the parameters of the barrier material. It should then behave more like an exciton of the embedding barrier material than that of the disc material. This also implies that the exciton could have energies (kinetic and correlation) significantly different from those of the 'normal' exciton within a conventional quantum well.

It has been pointed out by Le Goff and Stebe [5] that their results revealed that the peak position of the binding energy as a function of R does not depend strongly on the value of L, which is consistent with our present results. Here, we would like to add that the peak position of the binding energy as a function of L also remains fairly constant for different values of $R > 20$ Å. However, for the case of $R = 10$ Å (where the quasi-2D case is again restored) it is interesting to note that the peak position of the binding energy as a function of L shifted towards $L \simeq 40$ Å. We believe that this is due to the exciton behaving more like a barrier-material exciton as explained above. However, for the situation of the restored quasi-1D behaviour (when $L < 30$ Å), a corresponding shift of the peak position as a function of R is not obvious. This could probably be explained by the rate of recovery to the higher dimensionality, by looking at the decrease in the binding energy. The restoration of the quasi-2D behaviour was rather rapid as can be seen from the large drop in binding energy; while the restoration of the quasi-1D behaviour is much more gradual. This means that the shift in the peak position for binding energy as a function of R could still be observed for much smaller values of L than shown in the present results.

The position of the peak binding energy can hence be estimated to occur around $L \simeq 30$ Å and $R \simeq 20$ Å (or diameter ~ 40 Å) for the quantum disc or cylindrical quantum dot. It has been shown in reference [24] that there is a scaling rule for circular and square quantum wires of the form $L/(2R) = 0.9136$ such that a square wire of width L is equivalent to a circular wire of diameter $2R$, if the ratio of 0.9136 is achieved. Using this scaling rule, the critical confinement width for quantum square boxes, which are equivalent to the present quantum cylinders, can be estimated to be about $L \sim 36$ Å. From the behaviours of the peak binding energy position discussed above, we may conclude that the bulk effect sets in along any one spatial axis (dimension) at around ∼40–30 Å, fairly independently of the confinement conditions for the rest of the spatial dimensions. The present results should be useful for designers of nanoscale devices.

3.2. Virial theorem number

The results of Rossi *et al* [22] suggest that there is a constant virial theorem value of 4 for quantum wires of different shapes and sizes. This was concluded from their calculation which shows that for quantum wires in the strong-confinement regime, a universal scaling of the mean potential and kinetic energy exists with a potential-to-kinetic-energy ratio (E_C/E_K) of approximately 4. One direct consequence of their interpretation is that for a given value of the effective Bohr radius $a = \langle\psi_{ex}|r_{3D}^{-1}|\psi_{ex}\rangle^{-1}$ in a quantum wire, there is no hope of further increasing E_b by tailoring the potential-to-kinetic-energy ratio through the geometry of the confining profile. However, this has been disputed by Zhang and Mascarenhas [24] who have performed variational studies of the exciton energies in the quantum wells and wires using an infinite potential barrier. Here, we would like to again examine this issue, using the current finite-confinement disc formalism, for quantum structures of various confining geometries, including the limiting case of the quantum dot.

In figure 4(a), we show the virial theorem values v for quantum discs of various values of R and L which are representative of the limiting cases of the quantum well, wire, and dot,

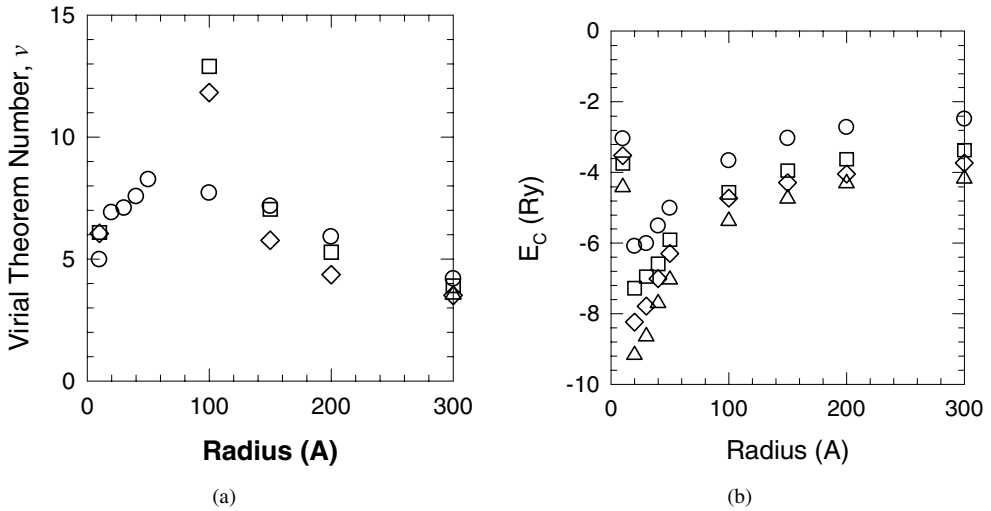

Figure 4. The virial theorem number v (a) and the Coulombic energy term E_C (b) are shown for various values of R and for $L = 300$ Å (circles), $L = 100$ Å (squares), $L = 30$ Å (triangles), and $L = 10$ Å (diamonds).

and in figure 4(b), the corresponding values of the Coulombic energy term E_C. Our present results in figure 4 again contradict the findings of Rossi *et al* [22]. In fact, there is no constant virial theorem number for the various geometries of the quantum structures considered here. This is consistent with the results of Zhang and Mascarenhas [24] who argued that the findings in [22] of different but constant virial theorem values for wells and wires are puzzling, since a realistic wire will evolve into a well or the bulk as the confinement is gradually relaxed. Here in figure 4, the virial theorem numbers are all larger than 2 and approach 2 in the limits where bulk effects are expected, except for the case of $R = L = 300$, where it has been shown [24] that v initially increases with the increase in L but subsequently decreases to approach 2 only at a wide well width of about 10 a_B ($\sim$1000 Å for the present material parameters). The reasons for the virial theorem numbers approaching 2 from above for the quantum wells have been well discussed by Zhang and Mascarenhas [24]. The physical origin of the nonconstant virial theorem value lies in the coexistence of single-particle confinement potentials with the two-particle Coulomb interaction.

To illustrate the behaviour of the virial theorem number for quantum wires, we again consider the regularized Coulomb potential $U = 1/(|z| + \gamma R/a_B)$ proposed by Banyai *et al* [2], where $\gamma = 0.3$ was found to yield a good fit to earlier more elaborate binding energy calculations. As the Schrödinger equation for such an effective potential yields bound-state wavefunctions which can be written in terms of the Whittaker functions [2], we may then use the ground-state wavefunction to calculate the energy terms, E_C and E_K, and hence the virial theorem number. We performed the calculations for R ranging between 0.1 and 1.0 a_B, and found that v is not a constant, but decreases from the order of 100 (for a small R) down to about 10.

Next, we would like to further examine the case of the quantum dot. In the strong-confinement regime of the quantum disc (R, $L \lesssim 100$ Å), the virial theorem number increases rapidly with decrease in R. This dramatic increase in v is due to both the increase in the magnitude of the Coulombic term (E_C) and the decrease in the kinetic term (E_K). As the spatial dimensions decrease, the magnitude of the Coulombic term increases rapidly; however, the kinetic energy of the exciton decreases as the relative motion of the electron and hole within the exciton becomes severely reduced. In an infinite confining potential, this motion eventually 'freezes out' in the limit of the quantum dot, while the Coulombic term diverges to infinity. Here, with the finite potential barriers, the magnitude of the Coulombic term behaves in a similar fashion to the corresponding binding energy; however, the kinetic energy could decrease to less than 10^{-2} Ryd, but rapidly increase to regain the bulk behaviour after the critical confinement limit. As the magnitude of Coulombic energy term could reach of the order of $\sim$10 Ryd, this means that the virial theorem number could then increase to over a hundred. In the present work, due to the heavy computation involved in calculating the fourfold integrals, the minimization with respect to the two parameters (α, γ) was carried out numerically with a precision of the order 10^{-2}; hence, we can no longer represent the virial theorem numbers accurately beyond this range. Nevertheless, the present results do show that the virial theorem number is in general not a constant for these cylindrical quantum dots of different sizes.

3.3. Fractional-dimensional parameter

It is worthwhile to note that the fractional-dimensional model for excitons originally sets out to provide a quantitative measure of the anisotropy of confined excitons (through the dimensionality parameter α_f) for various quantum structures. The dimensionality parameter with equation (18) was later used to calculate the binding energy of confined excitons in quantum wells and wires, by estimating the possible values of α_f for these structures. Although

the results obtained using this simplified calculation method were reasonably good [19, 20], the authors of [19, 20] have mentioned that the estimation of α_f remains somewhat heuristic. Hence, it would be of interest to back-calculate the values of α_f from the above binding energy results, to serve for future reference and comparison. In figure 5(a) we show α_f for quantum discs of various values of R and L calculated from equation (18). In a typical quantum well structure, we may immediately deduce that α_f should vary between 2 and 3. This is also the case for the present results for quantum discs of large radius ($R = 300$ Å), which approaches the quantum well situation.

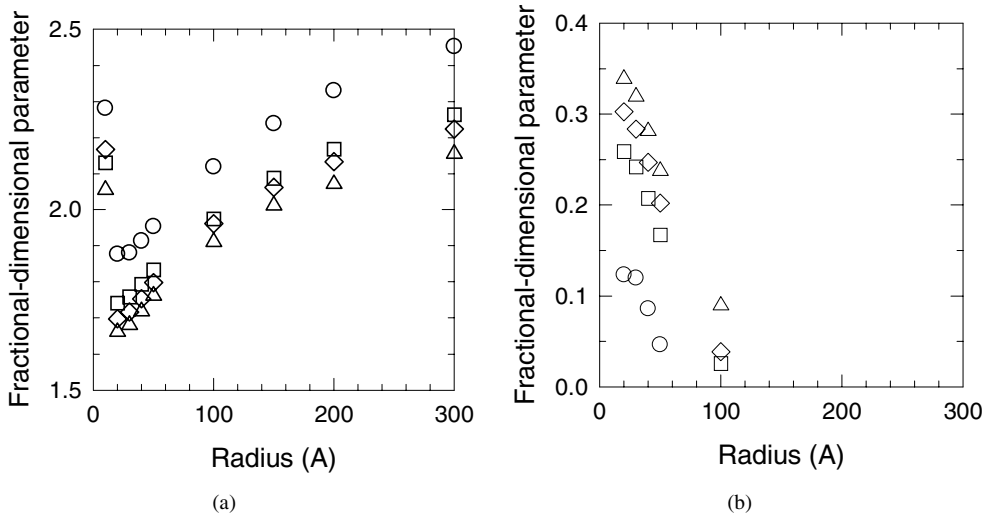

Figure 5. The dimensionality parameter α_f is shown for various values of R and for $L = 300$ Å (circles), $L = 100$ Å (squares), $L = 30$ Å (triangles), and $L = 10$ Å (diamonds). (a) As given by equation (18). (b) Assuming the negative root in equation (18).

However, the estimation of α_f for the quantum wire is less straightforward. We first note that for the ground-state exciton in a strictly 1D system, $\alpha_f = 1$ and the exciton binding energy diverges. As this could not be physically attainable for a realistic system, we expect α_f to be larger than 1. From figure 5, we also note that α_f-values around 2–2.2 are shared by quantum cylinders of $L = 300$ Å and quantum discs of $R = 300$ Å. This also implies the possibility that a narrow quantum well could have the same α_f-value as a quantum wire of larger R, as the excitons in these structures have about the same binding energy. This is in agreement with Christol *et al* [19, 20] who suggested $1 < \alpha_f < 3$ for the quantum wire, and also speculated that there could be common values of α_f for the quantum well and wires. As the same α_f now describes both the quasi-2D and quasi-1D situation, even for the present cases of the same material parameters, the question now arises as to whether α_f is a clear indicator of the anisotropy and dimensionality of the exciton in these structures. Hence we would like to remark that in order to lift this ambiguity between the well and wire, and to interpret α_f more effectively, it is necessary to know *a priori* the integer dimensionality (either 2D or 1D) which that of the structure most resembles.

As for the quantum dot, the open question now is whether α_f would cross the critical value of 1 if it were to vary continuously from 3 down to zero. One interesting observation from the present results is that α_f apparently does not deviate very much below 2, even for quantum discs of very small R and L ($\sim$30 Å), and quickly regains a value larger than 2 for very small R and L. Although this behaviour may be expected for the finite confinement, we have to further

examine the appropriateness of α_f as a dimensionality parameter. As discussed previously, the kinetic energy in the strong-confinement regime of the quantum discs becomes very small as the relative motion of the electron–hole pair is being reduced in all spatial directions. In such a situation, we should in principle classify them as quasi-0D structures. However, the values of α_f for these cases are obviously larger than 1, implying that these α_f-values could not represent the dimensionality appropriately. One may argue that the square root in equation (18) admits a negative value that could give an $\alpha_f < 1$. For these cases of 'negative roots', positive values of α_f exist for $E_b > 4$ Ryd. The α_f-values for the negative-root cases are plotted in figure 5(b). We note that such negative-root α_f-values could not render a good physical interpretation either. In the strong-confinement regime and before the bulk effect sets in, we should have a decreasing α_f as confinement further decreases, instead of α_f approaching 1 as is the case for these negative-root values. Considering the above discussion, we infer that α_f would not be able to adequately serve as a dimensionality constant for a realistic quantum dot.

Next, we examine whether α_f could function as an indicator of the anisotropy of the exciton in the quantum dot limit. We recall that the comparison of the variational results obtained using the isotropic (ϕ_1) and the present anisotropic (ϕ_3) trial wavefunctions seems to suggest a rather isotropic behaviour of the exciton in the limit of a small quantum disc. However, the exciton in such a situation is classified by a value of α_f of less than 2, which when interpreted in the usual sense as for the well and wire (i.e. when compared relatively to the 3D value of 3) indicates a high degree of anisotropy. It is understandable that the exciton is now very much compressed in the small quantum disc, but this compression occurs in all three directions which should not render it as 'very anisotropic'. In view of the above, if the fractional-dimensional model were to be applied to the exciton in the quantum dot, the usual interpretation of the fractional-dimensional parameter may not be adequate and it is necessary to have a new interpretation of α_f.

We would like to further mention the point made by Christol *et al* [19, 20] that no axiom in the basic formalism of the fractional-dimensional model strictly confines the dimensionality constant, α_f to be between 0 and 3. For example, in the case of the type II quantum well superlattice system where the carriers are confined separately in wide-gap and narrow-gap materials, the average spacing between the bound confined carriers along the growth direction may be larger than it is in the 3D crystal, which causes the binding energy to be smaller than Ryd. In this case, α_f becomes larger than 3 to account for this 'barrier screening' effect. We then have to question the physical significance of having a dimensionality or anisotropy greater than 3. In this regard, we tend to agree with Christol *et al* that α_f should be viewed more as a 'compression/dilation factor' (accounting for the spatial concentration of the wavefunctions) and not purely as an anisotropy or dimensionality parameter.

Lastly, we wish to point out that despite the above criticisms, the fractional-dimensional model does have several advantages, as it greatly simplifies the estimation of some important and useful parameters. In particular, the oscillator strength f_n of the nth confined exciton state can be quickly estimated [20] using

$$\frac{f}{f_{ex}} = \left(n + \frac{\alpha_f - 3}{2}\right)^{-3} \tag{20}$$

(where f_{ex} is the 3D exciton oscillator strength) once α_f is known.

4. Conclusions

The binding energy of an exciton in a quantum disc and the limiting cases were studied using a variational approach and the effective-mass approximation with a finite-confinement-potential

model. It was demonstrated that our two-parameter anisotropic trial wavefunction describes the exciton behaviour better than those used in previous calculations. Transitional behaviours between the quantum dot, wire, well, and bulk were studied in a continuous and unified manner. It was found that in various systems, an optimal confinement exists where the effects of quantum confinement are the largest. On the basis of these calculations, it was further shown that the dimensionality parameter α_f can be viewed more appropriately as a 'compression or dilation factor'. Our calculated results also disprove the recent claim that there exists a universal-constant virial theorem number for the quantum wells and wires.

References

[1] Bryant G W 1988 *Phys. Rev.* B **37** 8763
[2] Banyai L, Galbraith I, Ell C and Haug H 1987 *Phys. Rev.* B **36** 6099
[3] Kayanuma Y 1991 *Phys. Rev.* B **44** 13 085
[4] Brown J and Spector H N 1987 *Phys. Rev.* B **35** 3009
[5] Le Goff S and Stebe B 1993 *Phys. Rev.* B **47** 1383
[6] Le Goff S and Stebe B 1992 *Solid State Commun.* **83** 555
[7] Susa N 1996 *IEEE J. Quantum Electron.* **32** 1760
[8] Garm T 1996 *J. Phys.: Condens. Matter* **8** 5725
[9] Laheld U E H and Einevoll G T 1997 *Phys. Rev.* B **55** 5184
[10] Gerlach B and Wusthoff J 1998 *Phys. Rev.* B **58** 10 568
[11] Andreani L C and Pasquarello A 1990 *Phys. Rev.* B **42** 8928
[12] Zhu J, Zhu S, Zhu Z, Kawazoe Y and Yao T 1998 *J. Phys.: Condens. Matter* **10** L583
[13] Gotoh H and Ando H 1997 *Phys. Rev.* B **96** 1667
[14] Zheng R and Matsuura M 1998 *Phys. Rev.* B **56** 10 769
[15] Mosko M, Munzar D and Vagner P 1997 *Phys. Rev.* B **55** 15 416
[16] He X F 1987 *Solid State Commun.* **61** 53
[17] He X F 1990 *Solid State Commun.* **75** 111
[18] He X F 1991 *Phys. Rev.* B **43** 2063
[19] Mathieu H, Lefebvre P and Christol P 1992 *Phys. Rev.* B **46** 4092
[20] Christol P, Lefebvre P and Mathieu H 1993 *J. Appl. Phys.* **74** 5626
[21] Thilagam A 1997 *Phys. Rev.* B **56** 4665
[22] Rossi F, Goldoni G and Molinari E 1997 *Phys. Rev. Lett.* **78** 3527
[23] Thilagam A 1997 *J. Appl. Phys.* **82** 5753
[24] Zhang Y and Mascarenhas A 1999 *Phys. Rev.* B **59** 2040
[25] Marin J L, Riera R and Cruz S A 1998 *J. Phys.: Condens. Matter* **10** 1349
[26] Ben Daniel D J and Duke C B 1966 *Phys. Rev.* **152** 683
Bastard G 1988 *Wave Mechanics Applied to Semiconductor Heterostructures* (New York: Halsted)